Cell, Vol. 87, 447–458, November 1, 1996, Copyright ©1996 by Cell Press

A Complex of NuMA and Cytoplasmic Dynein Is Essential for Mitotic Spindle Assembly

Andreas Merdes,* Kasra Ramyar,‡ Janet D. Vechio,* and Don W. Cleveland*†
*Ludwig Institute for Cancer Research
†Division of Cellular and Molecular Medicine
University of California at San Diego
La Jolla, California 92093-0660
‡Johns Hopkins University School of Medicine
Department of Biological Chemistry
Baltimore, Maryland 21205

Summary

NuMA is a nuclear protein during interphase but redistributes to the spindle poles early in mitosis. To investigate its role during spindle formation, we tested spindle assembly in frog egg extracts from which NuMA was immunodepleted. Immunodepletion revealed that NuMA forms a complex with cytoplasmic dynein and dynactin. The depleted extracts failed to assemble normal mitotic spindles, producing, instead, chromatin-associated irregular arrays of microtubules lacking characteristic spindle poles. A subdomain of the NuMA tail was shown to induce microtubule aster formation by mediating microtubule bundling. Our findings suggest that NuMA forms bifunctional complexes with cytoplasmic dynein and dynactin that can tether microtubules at the spindle poles and that are essential for mitotic spindle pole assembly and stabilization.

Introduction

NuMA (nuclear/mitotic apparatus protein, also known as SPN, centrophilin, 1F1/1H1, SP-H, or W1) is a protein that accumulates at mitotic spindle poles, at or near the minus-ends of microtubules (Lydersen and Pettijohn, 1980; Yang et al., 1992; Kallajoki et al., 1991; Tousson et al., 1991; Compton et al., 1991; Maekawa et al., 1991; Tang et al., 1993). Several studies have indicated that NuMA might have a role in organizing or stabilizing the spindle apparatus. Microinjection of anti-NuMA antibodies into mitotic cultured cells led to the disruption of bipolar mitotic spindles (Kallajoki et al., 1991, 1992; Yang and Snyder, 1992; Gaglio et al., 1995). In some examples, NuMA could be found dispersed in the cytoplasm but still associated with one end of microtubule bundles. Furthermore, transfection of one dominant mutant form of NuMA that was unable to bind to the spindle (Compton and Luo, 1995) resulted in an aberrant spindle morphology with the polar regions losing their fusiform shape. These studies have raised the possibility that NuMA is involved in stabilizing the spindle poles, although NuMA is probably not directly associated with the centrosome. Immunoelectron microscopy of mitotic cells (Tousson et al., 1991; Maekawa et al., 1991) revealed that NuMA is localized in the polar region in a crescent-shaped area of high microtubule density but is not directly at the centrosome. In addition, the majority of NuMA does not colocalize with the centrosomal marker pericentrin (Compton et al., 1992; Kallajoki et al., 1992; Compton and Luo, 1995).

Besides its localization at mitotic spindle poles, NuMA is found in the interphase nucleus and may also have a function in postmitotic nuclear assembly, as indicated by antibody microinjection experiments (Kallajoki et al., 1991, 1993) and transfection of NuMA deletion mutants (Compton and Cleveland, 1993). In these studies, the formation of micronuclei was observed when affected cells tried to complete their mitotic cycle after apparently normal chromosome segregation in anaphase.

Although the previously described data appear consistent, their interpretation is complicated by the fact that all are based on the introduction of dominant and structurally disruptive antibodies or NuMA mutants. Evidence for the direct involvement of NuMA in spindle assembly and nuclear reformation has not been demonstrated. Very recently, however, Gaglio et al. (1995) did show that microtubule asters are formed in taxol-treated mitotic HeLa cell extracts containing NuMA, whereas extracts from which NuMA was immunodepleted failed in aster formation. Even though this process was clearly NuMA-dependent (because readdition of purified recombinant NuMA could restore aster formation), it is unclear to what extent these taxol-induced microtubule asters represent a model system for the assembly of functional mitotic spindles and spindle poles.

In this study, we now directly test the dependence of mitotic spindle formation on the presence of NuMA. We show that mitotic spindles assembled in frog egg extracts localize Xenopus NuMA (X-NuMA) to the spindle poles and that immunodepletion of the majority of NuMA blocks spindle formation, with microtubules attaching to chromosomes but failing to focus into a fusiform spindle.

Results

Cloning of the X-NuMA Homolog

To identify the structure of NuMA in frog, we used hybridization to the tail of human NuMA (Compton et al., 1992) to isolate an initial cDNA clone from a Xenopus laevis cDNA library. Successive rescreening and polymerase chain reaction–rapid amplification of cDNA ends yielded a set of overlapping clones from which the complete NuMA sequence was determined. This revealed an amino acid sequence of 2253 residues with a tripartite secondary structure, containing a 221 amino acid–long head domain, a discontinuous rod domain of 1563 amino acids, and a tail domain of 469 amino acids. The head region showed 49% identity to the human amino acid sequence; the degree of identity in the tail was 59%. Residues 2107–2112 (RQQMKR, Figure 1C) are homologous to the nuclear localization signal RQQRKR identified in human NuMA (Tang et al., 1994). The predicted coiled-coil helical domain is structurally very similar to human NuMA, although the sequence is only 37% identical.

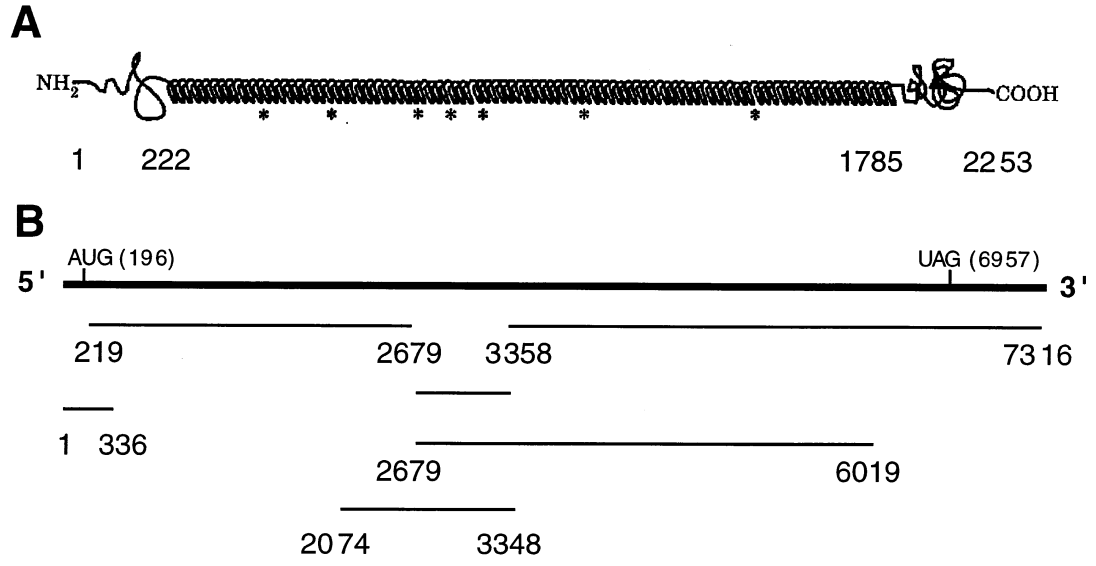

C

```
H-NuMA  MTLHATRGAALLSWVNSLHVADPVEAVLQLQDCSIFIKIIDRIHG-TEEGQQILKQPVSERLDFVCSFLQKNRKHPSSPECLVSAQKVLEGS--ELELAKMTMLLLYHSTMSSKSPRDWE  117
X-NuMA  MTSHSGKMEALLCWVNSLKVDEPIERFSQLQDLSILLKVVGVLSGNSEETAPVLQQDLEQRLNCLGSFLQRYCQTGSSAQNLVQWQKILQGENLEVELSKVIVILFYYSTMSSKNPRKSE  120

H-NuMA  QFEYKIQAELAVILKFVLDHEDGLNLNEDLENFL-QKAPVPSTC--SSTFPEELSP-PSHQARKEIKFLELQKVASSSSGNNFLSGSPASPMGDILQTPQFQMRRLKKQLADERSNRDEL  233
X-NuMA  DIDHKTQTELASILRFVLDNEDALCLDDKLINFLKRKAPFPSSGNDPSSSSDAMTPNVSHRRKSEVRFLQLHSVASSSTVKSLSADAPSSPMIEVLHTPQFQMRRLKKQLSEVRECRDEL  240

H-NuMA  ELELAENRKLLTEKDAQIAMMQQRIDRLALLNEKQAASPLEPKELEELRDKNESLTMRLHETLKQCQDLKTEKSQMDRKINQLSEENGDLSFKLREFASHLQQLQDALNELTEEHSKATQ  353
X-NuMA  EVELAENRKHLAEKEAQISLLQQQIENLRILRENQTELQ-EPKELEELRKNNESLMIRLRDTLKQCQDMKADKLLERKNDQLAEENGELSYKVRDLSNRLAQLQEALYETTEEQELSLS  359

H-NuMA  EWLEKQAQLEKELSAALQDKKCLEEKNEIIQGKLSQLEEHLSQLQDNPPQEKQEVLGDVEQETLKQEAATLAANNTQLQARVEMLETERGQQEAKLLAERGHFEEEKQQLSSLITDLQS  473
X-NuMA  NWQQKQNQLESELSGAVGEKKYLEEHNLILQGKISMLEDQLKEMGEIDMPETGDCMGDILKIDDLKQELAVLNTQCLSLKEQIHQMEEEKSTAEVEMEAQKSRFESEKGQLQEIVTNLQT  479

H-NuMA  STSNLSQAKEELEQASQAHGARETAQVASLTSELTTLNATIQQQDQELAGLKQQAKEKQAQLAQTLQQQEQASQGLRHQVEQLSSSLKQKEQQLKEVAEKQEATRQDHAQQLATAAEERE  593
X-NuMA  SLSEITFQKERLDNEARAQQEHLMCQITTLKLEISKLKSSLVHKDEELKGIHHKVEEE----------------RNEKNQLLENFKMLGGNLIGITQQLESK----TKEVDYLREQQQ  577

H-NuMA  ASLREEDAALKQLEALEKEKAAKLEILQQQLQVANEARDSAQTSVTQAQREKAELSRKVEELQACV-----------ETAFQEQHEA------QAQVAELELQLRSEQQKATEKERVAQ  695
X-NuMA  KILCERDSTLSTLNEYKCKKDENSGVLNKTVKTLEQDHQTSLSVIEKLKSEKEELASKVQDLDAKMLGLIAKCQNLDSENDSQSKSHAATVESLKAQLSEQESQLKIYRKKVSSNELVSE  697

H-NuMA  EKDQLQEQLQALKESLKVTKGSLEEEKRRAADALEEQQRCISELKAETRSLVEQHKRERKELEEERAGRKGLEARLLQLQEAHQAETEVLRRELAEAMAAQHTAESECEQLVKEVAAWRD  815
X-NuMA  ENSKLKDQLLSVEESLRHLREHLEKEKTKFAASLDADLKRISHLEEEMKKLSESRDEALHNLDEERTAGKKIESQLKHLEEEYQKANESLQAKLAGSCAAIKQREERDELSKVVDIWKA  817

H-NuMA  GYEDSQQEEAQYGAMPQEQLMTLKEECEKARQELQEAKEKVAGIESHSELQISRQQNKLAELHANLARALQQVQEKEVRAQKLADDLSTLQEKM----AATSKEVARLETLVRKAGEQQE  931
X-NuMA  KYGESQQKIAQNSCHMQEQTEELKKTHSDVYQQLEGERSVLMIEAKASETKSSQLEKINQLEGELSAANACIKERENAEEKKLVSALHSAEEKLKIAYQGESERLSHLETALSNAKQDLD  937

H-NuMA  TASRELVKEPARAGDRQP--EWLEEQQGRQFCSTQ-------AALQAMEREAEQMGNELERLRAALMESQGQQQEERGQQEREVARLTQERGRAQADLALEKAARAELEMRLQNALNEQR  1042
X-NuMA  CLAKELSDEKYKKAEFEAMVKVLKEQNSERIASLESELKNSLAVVKERKCESEKLSGEVEHLKRQLDDSSQKHKEALAQKNIEIKQLINAKEKATSDLAI----KSEMGAQLQKAVDTHK  1053

H-NuMA  VEFATLQEALAH----------------------------------------------------ALTEKEGKDQ---------ELAKLRGLEAAQIKELEELRQTVKQLKEQLAKKEKEHAS  1103
X-NuMA  SEFSALQNELSRSLDLLALKEGEVERLNKEAALRQEEIQQQQQTITKLTEEETALAALKDKVALQEKEIKQQVQATKGAEKEMAKLKSVISEKSKRIECLEQDIQNQKRDLSCIQEQHQS  1173

H-NuMA  ---------------------------------GSGAQSEAAGRTEPTGPKLEALRAEVSKLEQQCQKQQEQADSLERSLEAERASRAERDSALETLQGQLEEKAQELGHSQSALASAQRE  1191
X-NuMA  KLGESQGLQALIADLEKKCKEQKELICEAQNKAAEAKTLASEKASVSERQLEGIQA----LEIEIGKERQKACDLQKQLELSWAVQEEKETELQALKKELFHKVQELEQSQTSFTDSSGE  1289

H-NuMA  LAAFRTKVQDHSKAEDEWKAQVARGRQEAERKNSLISSLEEEVSILNRQVLEKEGESKELKRLVMAESEKSQKLEESCACCRQRQPATVPEL--QNAALLC-GRRCRASGREAEKQRVAS  1308
X-NuMA  ALLYLSEAQERQQALTEAKFQAEQYQKEIEMKNKEVNSLQAEIKILSSKVTTNEEVSVDFEQRLLKETSKSAKLEEKMQKLHMELEASFKELLEKNCAIDCLTTEAQNLKGEADQQRMAV  1409

H-NuMA  ENLRQELTSQAERAEELGQELKAWQEKFFQKEQALSTLQLEHTSTQALVSELLPAKHLCQQLQAEQAAAEKRHRSELEQSKQAAGGLRAELLRAQRELGELIPLRQKVAEQERTAQQLRA  1428
X-NuMA  DSLQQKLSSKAETNHTLQQEIQAWQKNCAEKEQQICSLQQNLKSNQSLLEEFASLKHSYQEIIAERDLMQEKHQEELLSHKKLTERFQAELEKAKEDMTEIVLLKEKLHNQELQLHKFQS  1529

H-NuMA  EKASYAEQLSMLKKAHGLLAEENRGLGERANLGRQFLEVELDQAREKYVQELAAVRADAETRLAEVQREAQSTARELEVMTAKYEGAKVKVLEERQRFQEERQKLTAQVEELSKKLADSD  1548
X-NuMA  ENSYSLTQISHLQQVNSQLLGANQSLSQISDQGAKKLESEMSTLKEQHKEEMKTLRLQYEKTLREGNKQVQETSLQLETVTSKYDHVKSKVLKDQKTFQEEKQRLLLQVQELNKQLSQQE  1649

H-NuMA  QASKVQQQKLKAVQAQGGESQQEAQRFQAQLNELQAQLSQKEQAAEHYKLQMEKAKTHYDAKKQQNQELQEQLRS----LEQLQKENKELRAEAERLGHELQQAGLKTKEAEQTERHLTA  1664
X-NuMA  KTIRSQQQKLK---QREGETHEEADKSHKRVLELESQLEQQTQAVEHYKAQMEKAKVHYDAKKQNQELSEELQSHIKQQEHLSKENADLKAESEQLHKELQHSLLQSKEVEQNCKNLSN  1766

H-NuMA  QVRSLEAQVAHADQQLRDLGKFQVATDALKSRE-----PQAKPQLDLSIDSLDLSCEEGTPLSITSKLPRTQPDGTSV-PGEPASPISQRLPPKVESLESLYFTPIPARSQAPLESSLDS  1778
X-NuMA  RVRSLEASWSTLTGQLRDPGKFQLATAFHEESGHFCAPRQTRSHADVSIDSLDLSFGEDQLLNSTSERCNEEPATSSVHASSPDSLISGQLPKKVESLESLYFTPIPTRAQSKLESSIGS  1886

H-NuMA  LGDVFLDSGRKTRSARRRTTQIINITMTKKLDVEEPDSANSSFYSTRSAPASQ----------ASLRATSSTQSLARLGSPD--------YGNSALLSLPGYRPTTRSSARRSQAGVSSG  1880
X-NuMA  IGDLSLDSSKKTQSARRRTMQIINITMTKKTK-EEPESANTSFYSLRSAPSVQSLHLQNPRRAGRPPAAISAPAIASLPSQESLAKTEHFSSDDSLNNLPGVQHPTRRSARLSQTG----  2001

H-NuMA  APPGRNSFYMGTCQDEPEQLDDWNRIAELQRNRVCPPHLKTCYPLESRPSLSLGTTTDEEMKTGDPQETLRRASMQPIQIAE----------GTGITTRQQRKRVSLEPH  1981
X-NuMA  ---GRSSFYMSTCQDEPDPQDDWTRIAELQARNKTCPPHLKTSYPLESRPSIFSSTITDEEVKLGDPKETLRRATLLPQQIQDSMTSTRRQTLAVPGAEHLKGHNISTFQQMKRVSEESH  2118

H-NuMA  QGPGTDESKKATSCFPRPMTPRDRHEGRKQSTTEAQKKAAPASTKQADRFQSMAFSILNTPKKLGNSLLRRGASKKALSKASPNTR----------SGTRRSPRIATTTA  2081
X-NuMA  YGPDTPEAKKTATCFPRPMTPKDKHDTRRVSTMES-KGSSSHQQAQPTRRQATAFSIFNTPKKLGNSLLKRGLNKKTTPKNSPRGRGANGSTSSTSNKPSHLSLRKSPSQRSPRVSTAKS  2237

H-NuMA  SAATAAAIGATPRAKGKAKH    210
X-NuMA  PRASNKLFE---RKQQRNK-    225
```

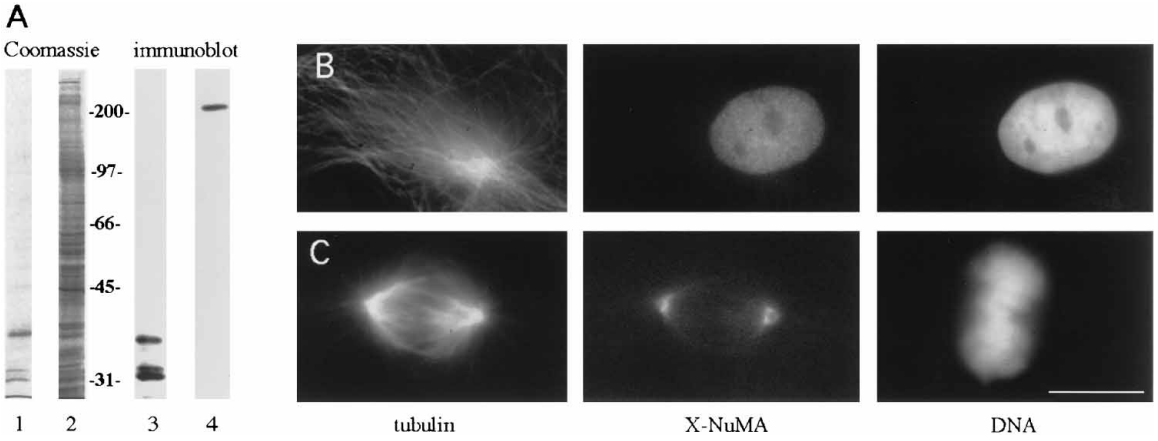

Figure 2. X-NuMA Localizes to Interphase Nuclei and Mitotic Spindle Poles

(A) (Left) Coomassie-stained protein gels loaded with a NuMA-tail fusion protein purified from bacteria (lane 1) or total Xenopus laevis egg extract (lane 2). (Right) the same gels immunoblotted with anti–NuMA-tail antibody.

(B) NuMA (middle) localization to the nucleoplasm of an interphase Xenopus A6 cell. (Left) tubulin staining of the same cell; (right) DNA visualized by DAPI staining.

(C) Localization of NuMA (middle), tubulin (left), and DNA (right) in an A6 cell at metaphase. Scale bar, 10 μm.

Antibodies against NuMA Coimmunoprecipitate a Cytoplasmic Dynein–Containing Complex

To raise specific anti-Xenopus NuMA antibodies, hexahistidine-tagged fusion proteins encoding amino acid residues 627–1051 and 1994–2253 were expressed in bacteria, purified over Nickel-agarose columns, and injected into rabbits. These antibodies recognized the full-length NuMA protein in frog egg extracts by immunoblot (Figure 2A, lane 4) and by immunofluorescence gave a typical nuclear staining in interphase-cultured Xenopus A6 cells (Figure 2B) or decorated a crescent-shaped pattern at the spindle poles of mitotic cells (Figure 2C).

When demembranated Xenopus sperm chromatin was incubated with Xenopus egg extract, microtubule asters around the sperm centriole were formed within 15 min. As shown in Figure 3A, these structures formed without detectable quantities of NuMA on or around the sperm DNA. Only a diffuse staining of NuMA was faintly visible in the area of the radial microtubule arrays. After 30–40 min, the aster-like microtubule pattern was reorganized into an asymmetric half-spindle–like morphology, as previously described (Sawin and Mitchison, 1991; Sawin et al., 1992a). At this point, NuMA could be found concentrated at the poles of these half-spindles but only at the side facing the sperm DNA (Figure 3B).

Frog egg extract was then cycled through interphase (by addition of 0.4 mM calcium chloride to trigger proteolysis of cyclin and a drop in cdc2 activity). As a consequence, the sperm chromatin decondensed, a nuclear envelope formed, and DNA replication initiated. During this interphase, NuMA was concentrated in the nuclei that had formed from the demembranated sperm (Figure 3C). After 80–90 min of incubation, when cdc2 levels rose as a consequence of cyclin synthesis, condensation of the chromatin was reinitiated and the NuMA staining disappeared from the nucleus (Figure 3D). Upon readdition of cytostatic factor (CSF)–arrested extract, mitotic spindles formed in vitro that were stably arrested in a metaphase state. NuMA was highly concentrated at the spindle poles (Figure 3E), as in mitotic spindles in tissue culture cells (see Figure 2C).

To test whether NuMA was essential for the formation of mitotic spindles or microtubule asters or both, we immunodepleted it from mitotic frog egg extracts, using anti-NuMA antibodies bound to protein A beads. Immunoblots (Figure 4A) revealed that untreated extracts (lane 1) and mock-depleted extracts (lane 2), incubated with irrelevant control IgG beads, both contained equivalent levels of the NuMA protein. With a dilution series of known amounts of recombinant NuMA tail, the concentration of NuMA in frog egg extracts was quantified by dot-blotting and immunoblotting to be between 8 and 14 μg/ml (depending on the method used), corresponding to approximately 0.01% of total extract protein (70–80 mg/ml). In mitotic extracts that were incubated with anti-NuMA tail–protein A beads, practically all NuMA could be depleted (Figure 4A, lane 3) and could be quantitatively recovered from these beads in a single low pH step (Figure 4B, lane 3). Examination of the immunoadsorbed material by gel electrophoresis and Coomassie staining (Figure 4C, "Coomassie") revealed a prominent band above 200 kDa that immunoblotting

Figure 1. Structure of X-NuMA

(A) X-NuMA is comprised of globular head and tail domains, connected by a large α-helical rod domain that is partly interrupted by short nonhelical stretches (indicated by asterisks).

(B) Sequence of X-NuMA determined from six overlapping cDNA clones.

(C) Alignment of Xenopus (X-) and human (H-) NuMA polypeptides. Identical amino acid residues are on a shaded background. The nuclear localization signal is underlined in H-NuMA. Nucleotide and amino acid sequence data are available from EMBL/Genbank under accession number Y07624.

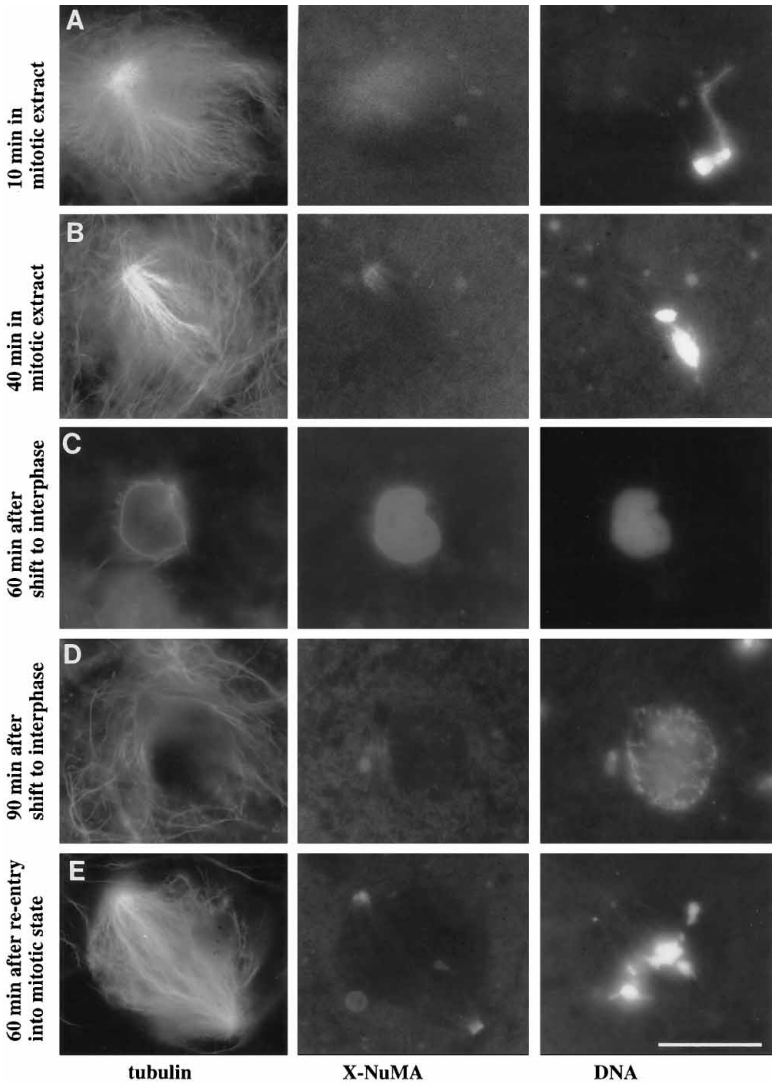

Figure 3. Cell Cycle–Dependent Localization of NuMA to Microtubule Asters in Nuclei and on Mitotic Spindles Assembled In Vitro

Microtubule assembly, NuMA localization, and DNA position were monitored for (A) 10 min or (B) 40 min following addition of sperm nuclei to mitotic extract, (C) 60 min or (D) 90 min following addition of Ca^{2+} to shift the extract into interphase, or (E) 60 min following entry into a second mitotic state by addition of fresh CSF extract. (Left panels) microtubule arrays visualized with rhodamine-tubulin; (center) NuMA visualized by indirect immunofluorescence with a NuMA antibody and a fluorescently labeled secondary antibody; (right) DNA visualized with DAPI. Scale bar, 20 μm.

confirmed to be NuMA (data not shown). Besides NuMA, additional bands at approximately 500 kDa, 150 kDa, and 90 kDa were also removed by the anti-NuMA tail antibody, suggestive of a NuMA-containing protein complex. The idea of a specific complex of coprecipitating proteins was further supported by the use of a second anti-NuMA antibody raised against a nonoverlapping sequence in the rod domain. This antibody also depleted NuMA as well as the 90, 150, and 500 kDa species, whereas control IgGs did not precipitate any of these bands (see top panel of the Coomassie-stained gel in Figure 4C).

As to the identity of the coprecipitating polypeptides, the large size of the 500 kDa band (comigrating along with Xenopus cytoplasmic dynein heavy chain; Figure 4C, "Coomassie") suggested it might represent cytoplasmic dynein heavy chain, which is known to exist in a complex with a 70–90 kDa intermediate chain and several 60–70 kDa light chains (see also Niclas et al. [1996] for a recent description of dynein in frog eggs). Immunoblotting with an antibody against Dictyostelium dynein heavy chain (Koonce et al., 1992), affinity-purified over nitrocellulose strips of electrotransferred Xenopus dynein, indicated that the 500 kDa band is cytoplasmic dynein heavy chain (Figure 4C, "anti-dhc"). Further, immunoblotting with an anti-dynein intermediate chain antibody (monoclonal antibody [MAb] 70.1) revealed that dynein intermediate chain is also specifically coprecipitated with both anti-NuMA antibodies but not in controls (Figure 4C, "anti-dic"). The 150 kDa species, which is another specific coimmunoprecipitate, shows a similar electrophoretic mobility as p150/glued, a polypeptide of the dynactin complex proposed to activate dynein-dependent motility (Gill et al., 1991; Schroer and Sheetz, 1991). Immunoblotting with a monoclonal anti-p150/dynactin antibody (Figure 4C, "anti-dynactin"; MAb 150 B) confirmed that dynactin is a component of the NuMA precipitate.

To examine the composition of the NuMA-containing complex in more detail, following initial removal of nonspecifically bound proteins with buffer and detergent, the immunoprecipitates were incubated in buffer containing 0.5 M NaCl (Madine et al., 1995). Under these conditions, the dynein/dynactin components were

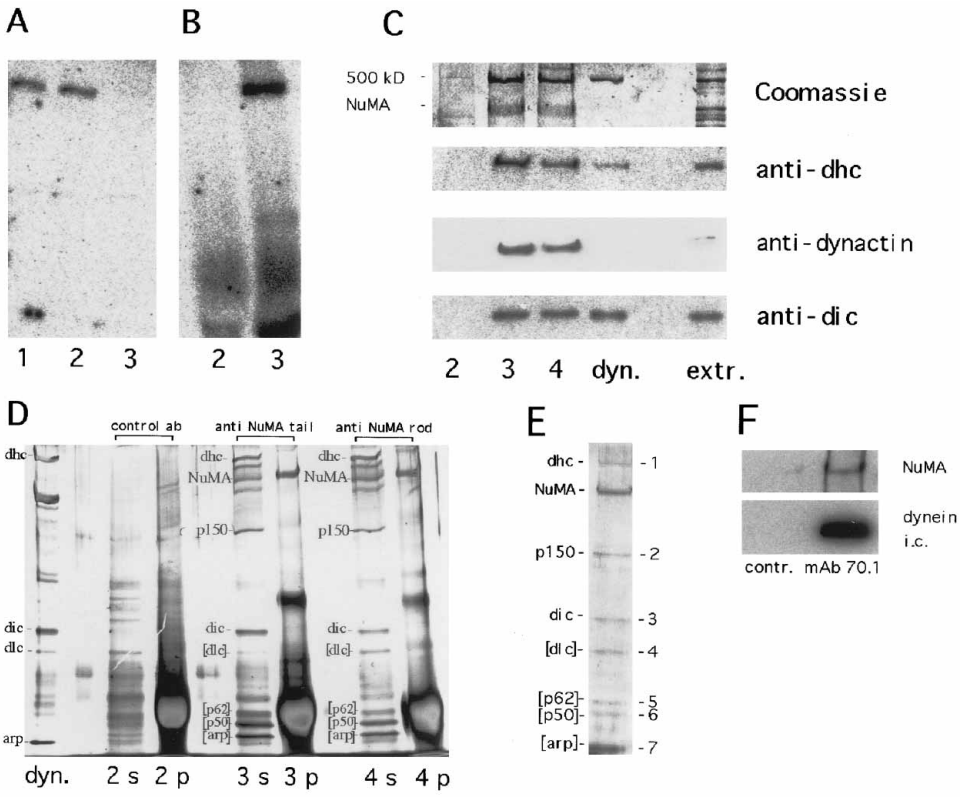

Figure 4. Depletion of NuMA from Egg Extracts Reveals Association of NuMA with Cytoplasmic Dynein and Dynactin

(A) Immunoblot for NuMA in untreated egg extract (lane 1), mock-depleted extract using a commercial rabbit anti-mouse IgG (lane 2), and extract following immunodepletion with anti–NuMA-tail antibody (lane 3).

(B) Immunoblots for NuMA of proteins immunodepleted from extracts using anti-NuMA tail antibody (lane 3) or control antibodies (lane 2).

(C) Coomassie: portion of a Coomassie-stained gel, showing the immunoprecipitates from mock-depletion (lane 2), anti-NuMA tail antibody depletion (lane 3), anti-NuMA rod antibody depletion (lane 4), cytoplasmic dynein–enriched Mg-ATP eluate from taxol-stabilized microtubules in frog egg extract (dyn.) and Xenopus egg extract (extr.). anti-dhc: immunoblot of an identical gel, probed with anti-dynein heavy chain antibody. anti-dynactin: immunoblot probed with anti-p150 glued/dynactin antibody. anti-dic: immunoblot probed with anti-dynein intermediate chain antibody.

(D) Silver-stained gel of immunoprecipitates eluted with a high salt buffer, from mock (2 s), anti-NuMA tail (3 s), and anti-NuMA rod (4 s) antibody depletions. Equivalent sample volumes of the corresponding pellets are shown in lanes 2 p, 3 p, and 4 p. Lane dyn. contains material as described in Figure 4C. The migration positions of dynein heavy chain (dhc), NuMA, p150 glued/dynactin (p150), and dynein intermediate chain (dic), as well as the putative positions of dynein light chain (dlc), dynactin p62 (p62), dynactin p50 (p50), and the actin-related protein arp1 (arp) are indicated in the figure.

(E) Coomassie-stained gel showing the NuMA–dynein–dynactin complex after immunoadsorption from frog egg extract with an anti-peptide antibody against a NuMA tail sequence and elution with an excess of NuMA tail peptide.

(F) Immunoblots of anti-dynein intermediate chain (MAb 70.1) and rabbit IgG (contr.) immunoprecipitates, probed with anti-NuMA (top) and anti-dynein intermediate chain (bottom).

eluted (Figure 4D, lanes 3 s and 4 s), whereas the majority of NuMA (as well as a diffusely staining protein band above 100 kDa and the NuMA antibody) remained still firmly bound (Figure 4D, lanes 3 p and 4 p). The eluates of both anti-NuMA rod and tail antibody precipitates showed an identical protein band pattern, comprising the above characterized bands of dynein heavy chain (approximately 500 kDa), p150 glued/dynactin (150 kDa), dynein intermediate chain (approximately 90 kDa), and a group of four bands of molecular masses between 45 and 65 kDa. Although no antibodies are available that react with the frog homologs, these additional bands have molecular masses and stoichiometries appropriate for other components of the dynein motor complex, including the dynein light chains (approximately 60 kDa; compare with the protein bands from partially purified dynein in Figure 4D, lane dyn), and three additional components of the dynactin complex, including the actin-related protein arp1 (approximately 45 kDa), as well as p50 and p62 (not visible in lane dyn, because the majority of the dynactin components did not copurify with frog egg dynein by ATP–elution of microtubules). A set of two additional weak bands of sizes between 200 and 400 kDa were only visible after silver staining and were not consistently seen in all immunoprecipitation experiments (compare with Figure 4C, "Coomassie"), probably representing degradation products of dynein heavy chain or NuMA, respectively. (NuMA degradation products of 180–200 kDa are occasionally detected in immunoblots of frog egg extracts; data not shown).

To confirm the existence of the NuMA–dynein–dynactin complex and to purify it in a native form, we

prepared an antibody against a NuMA-tail peptide, coupled it to protein A beads, and used these to immunoadsorb the complex from a mitotic frog egg extract. NuMA and associated proteins were specifically eluted by the addition of an excess of the peptide. Figure 4E shows that the recovered NuMA coeluted with the same seven dynein/dynactin polypeptides as described in the previous experiments, although the amount of associated dynein was at somewhat lower stoichiometry compared with the yield using the polyclonal anti-rod and anti-tail antibodies. It is possible that this particular antipeptide antibody interferes partially with the binding of the dynein–dynactin complex or that losses of dynein/dynactin occurred during the isolation procedure.

To obtain an estimate of the molar ratio between dynein and NuMA in the immunoadsorbed complex using polyclonal anti-NuMA rod and anti-NuMA tail antibodies, we determined the relative amounts of both proteins by scanning of Coomassie-stained gels. In both immunoprecipitates, NuMA was present in an approximate molar ratio of 1.6 ($\pm$ 0.5) compared with dynein heavy chain (determined from six different experiments). In the initial frog egg extracts, however, the amount of dynein clearly exceeded the amount of NuMA by approximately 30:1; consistent with this, NuMA-depleted extracts still contained an essentially undistinguishable amount of dynein heavy chain polypeptides (data not shown). Also, p150 glued/dynactin was present in significant excess over NuMA in frog egg extracts (data not shown).

For a final verification of the association between NuMA and dynein with an independent approach, dynein intermediate chain was immunoprecipitated (with the antibody MAb 70.1) from egg extracts, and the precipitates were assayed for NuMA (Figure 4F). This revealed that NuMA was coprecipitated as expected for a NuMA–dynein complex. To test whether other, nondynein, microtubule-dependent motors were also part of the NuMA complex, we blotted NuMA immunoprecipitates with antibodies to two broadly conserved domains in kinesin-like proteins (anti–LAGSE and anti–HIPYR peptide antibodies; Sawin et al., 1992b). No specific reactive bands were identified.

These data indicate that a well-defined complex of NuMA and at least seven additional polypeptides (marked 1–7 in Figure 4E), comprising dynein and dynactin components, can be coimmunoprecipitated from frog egg extract.

Depletion of NuMA Inhibits Spindle Formation But Not Assembly of Mitotic Asters

To examine the consequences of NuMA depletion, mitotic extracts were incubated with demembranated sperm. After incubation for 15–30 min at room temperature, in both control (Figure 5A) and depleted (Figure 5B) extracts, radial microtubule asters formed around the sperm centrosome, indicating that the initial process of microtubule nucleation and growth is a NuMA-independent process. Incubation of the extracts was continued for approximately 75 min, a time sufficient to allow bipolar mitotic spindle assembly in control samples (Figure 5C; see also Sawin and Mitchison, 1991). On the other hand, removal of NuMA from the extracts resulted in a dramatic morphological disruption of spindle assembly; in depleted extracts, although microtubule assembly was not inhibited, microtubules were not organized from spindle pole-like foci (Figure 5D, top). Instead, the microtubules were found in disorganized arrays juxtaposed with condensed DNA (Figure 5D, bottom). The morphology of these aberrant structures was reminiscent of nonfusiform spindle fibers that were not regularly bundled and lacked a pole. In addition, the majority of these structures were about 1.5 times larger than normal spindles (as determined by the distance between opposing microtubule ends; see Figures 5D, 5F, 5H, and 5J, as well as Figure 6B). The same phenotype could be observed in NuMA-depleted extracts cycled through interphase and driven back into mitosis (Figure 5F), while mock-depleted control extracts (Figure 5E) remained fully competent to form bipolar spindles and to segregate chromosomes when the metaphase-to-anaphase transition was triggered by influx of calcium (Shamu and Murray, 1992).

To quantitate the effects of NuMA depletion on spindle assembly, we determined the percentage of spindles formed per nucleus in extracts at various concentrations of NuMA. For this purpose, NuMA-depleted CSF–arrested extract was mixed with undepleted extract at different ratios, and spindle formation was observed after 1.5 hr incubation with sperm DNA. When 90% of the NuMA protein was depleted, only 2% of the chromatin was organized in bipolar spindles (10 spindles/583 nuclei). All other DNA was surrounded by abnormal microtubule structures, as shown in Figures 5D, 5F, 5H, and 5J. At NuMA concentrations of 55% or 75% of the original value, 19% (30 spindles/157 nuclei) or 46% (119 spindles/258 nuclei) were counted, respectively. Undepleted extract, on the other hand, yielded 100% of added sperm DNA organized into bipolar spindle arrays (384 spindles/384 nuclei).

To investigate more closely the effect of NuMA depletion on the structure of the spindle poles and spindle pole components, we examined the localization of the centrosomal marker proteins pericentrin and γ-tubulin along with potential residual NuMA. To process samples for immunofluorescence, we spun the extracts onto glass coverslips. The abnormal microtubule arrays in NuMA-depleted extracts were very fragile and varied in their morphological appearance, probably owing to the centrifugation procedure. No obvious structures reminiscent of spindle poles could be found in depleted extracts, and NuMA (Figure 5H), pericentrin (Figure 5J), and γ-tubulin (data not shown) were absent from these aberrant assembly products; in contrast, control spindles contained NuMA and pericentrin localized in relatively well-defined regions at the poles (Figures 5G and 5I).

Readdition of NuMA to Depleted Extract Partially Rescues Spindle Formation

To test whether spindle assembly could be rescued by addition of purified NuMA to depleted extracts, we immunoadsorbed NuMA from frog egg extract to protein A beads coated with the antibody against the NuMA-tail peptide. NuMA and the dynein–dynactin complex

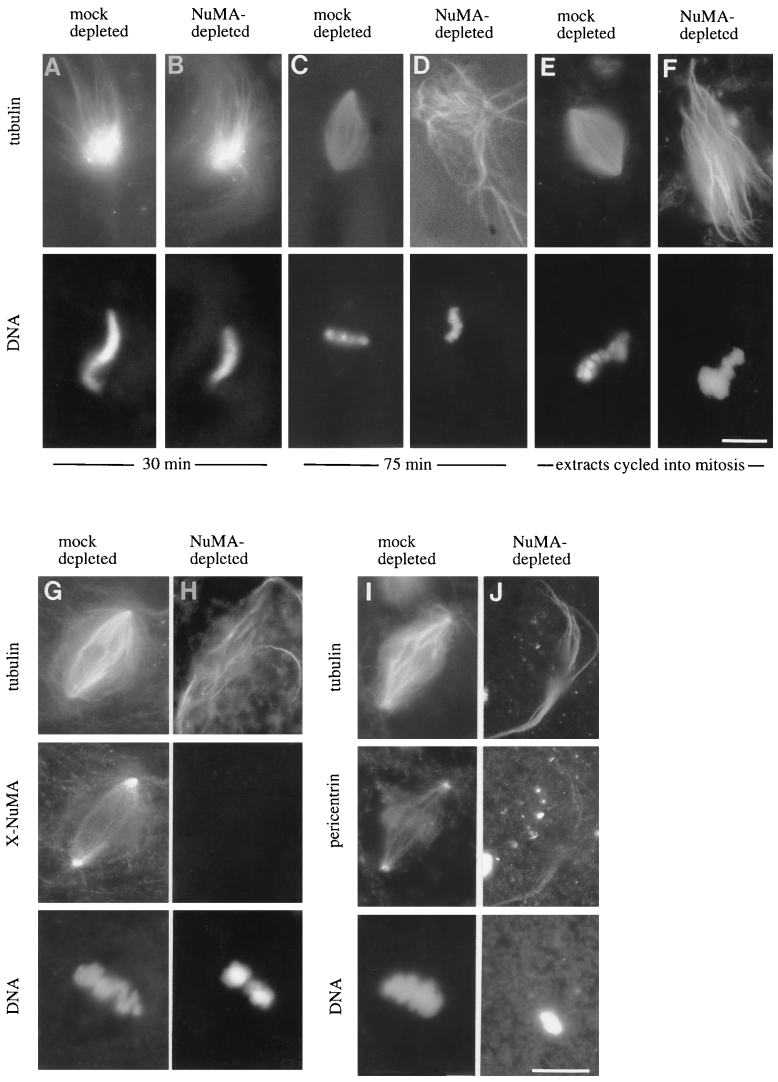

Figure 5. NuMA Is Required for the Formation of Bipolar Spindles and the Organization of Spindle Poles, But Not Mitotic Asters, In Vitro

Rhodamine-labeled tubulin and sperm nuclei were added to mitotic extracts, and aster formation or spindle assembly were assessed in (A, C, E) control or (B, D, F) NuMA-depleted extracts, 30 min (A and B) or 75 min (C and D) after sperm addition. In (E) and (F), mock-depleted (E) and depleted (F) CSF extracts were supplemented with sperm, and the mitotic block was released by Ca^{2+} addition. After 90 min in interphase, the extracts were driven into mitosis by addition of a half-volume of mock-depleted (E) or depleted (F) CSF extract, respectively. Upper panels: rhodamine-tubulin; lower panels: sperm DNA, stained with DAPI. (H, J) NuMA-depleted and (G, I) control extracts, cycled from interphase into mitosis, were monitored for spindle assembly as in (E) and (F). Extracts were spun onto coverslips and immunostained (middle panels) for X-NuMA (G, H) and pericentrin (I, J). (A)–(F) and (G)–(J) are shown at the same magnifications, respectively. Scale bars in (F) and (J), 20 μm.

were specifically eluted from these beads by the addition of an excess of the peptide (see Figure 4E). The isolated NuMA complex was concentrated and added to depleted extract to restore 70% or 150% of the original NuMA concentration (Figure 6E). Whereas depleted extracts (Figure 6B) yielded again almost exclusively long structures without poles (98%, 125/128 structures; the remaining approximately 2% were similar to half-spindles), 31% of the structures in restored extracts were monopolar half-spindles (28/90 structures, Figure 6D), indicating that addition of the NuMA complex successfully stimulated the first step seen in spindle assembly in undepleted extracts (see Figures 3A and 3B). Moreover, bipolar spindles were assembled in restored extracts (Figure 6C), although such bipolar structures were more fragile during centrifugation onto microscope coverslips than control spindles and represented less than 5% of the structures assembled. In comparison, no bipolar structures were ever seen in the depleted extracts. The remaining sperm DNA in restored extracts was found associated with poleless microtubule structures; however, in contrast to the much longer structures in depleted extracts, these were uniformly of comparable sizes to control spindles. Thus, the readded NuMA complex very efficiently suppresses the phenotype of unusually large aberrant microtubule structures found in depleted extracts, promotes pole formation in half-spindles, and partially restores bipolar microtubule structures. It is possible that the readded NuMA complex contains fewer proteins than the material removed by depletion or that the readded material is partially inactive, explaining why we could not obtain a full reconstitution.

In another reconstitution experiment, we tested whether purified recombinant NuMA, without associated dynein/dynactin components, was able to rescue spindle formation in depleted extracts. Because attempts at expressing recombinant Xenopus NuMA were unsuccessful, we chose to reconstitute depleted extracts with human NuMA (purified from insect cells infected with baculovirus encoding wild-type human NuMA; Figure 6F). After solubilizing the purified NuMA in 8 M urea and attempting to refold the protein by dialysis against phosphate-buffered saline (PBS), the human NuMA was added to depleted extracts at a final concentration of 1.5 times the amount of X-NuMA in the

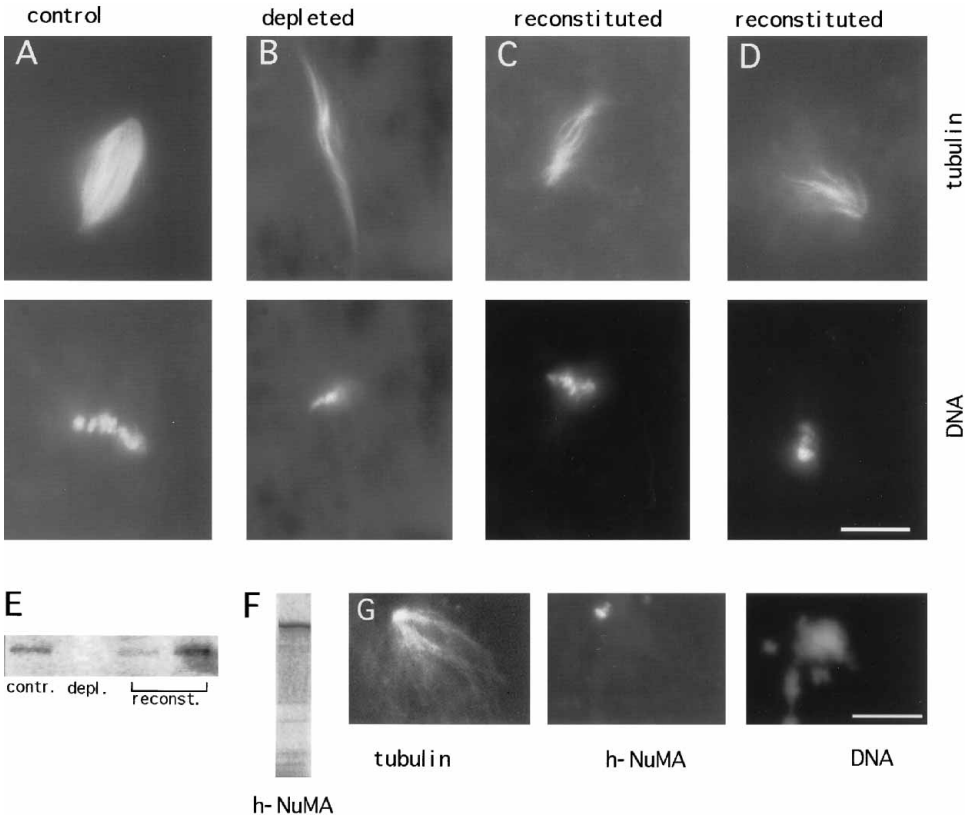

Figure 6. Spindle Formation in NuMA-Depleted Extracts Can Be Partially Rescued by the Addition of Immunoaffinity-Purified X-NuMA or Recombinant Human NuMA

(A) Mitotic spindle assembled after 1 hr in mock-depleted control extract (top) and corresponding picture of the DAPI–stained chromosomes (bottom).

(B–D) Microtubule structures (top) obtained in depleted extract (B) and reconstituted extract (C and D); DNA staining (bottom).

(E) Anti-NuMA immunoblot of control (contr.), NuMA-depleted (depl.), and reconstituted (reconst.) frog egg extracts.

(F) Recombinant human NuMA, purified from NuMA-encoding baculovirus-infected insect cells displayed on a 6% SDS–polyacrylamide gel electrophoresis gel.

(G) Depleted CSF–arrested mitotic extract supplemented with recombinant human NuMA to 10 μg/ml. Sperm incubation was performed in the presence of Ca^{2+}, and induction of mitosis was triggered by addition of CSF–arrested depleted extract. (Left) rhodamine-tubulin fluorescence; (middle) recombinant human NuMA, stained with a human NuMA-specific antibody; (right) DNA staining with DAPI. Scale bars in (D) and (G), 20 μm.

original (undepleted) extract. Human NuMA did promote the formation of half-spindles containing a focused pole region, with human NuMA localized in the pericentrosomal area (Figure 6G), although in this case none of these progressed to bipolar spindles.

While the reconstitutions with the X-NuMA complex or purified human NuMA only partially restored full spindle assembly (as was also the case in the only previously published attempt at spindle reconstitution in this system [Walczak et al., 1996]), both experiments demonstrate that NuMA is an essential component for the formation of convergent spindle poles and for maintaining the size and the shape of mitotic spindles.

A Portion of the NuMA Tail Domain Can Directly Bind to Tubulin

To understand the mechanism of NuMA-binding to spindle microtubules and the spindle poles, we incubated purified NuMA fusion proteins with Xenopus egg extract in the absence of sperm nuclei. Because previous studies had already suggested that the NuMA tail was important for the interaction with mitotic spindles, we further dissected the tail region by subcloning and expressing the proximal and the distal half of the tail (named tail I and II, respectively). As shown in Figure 7A, the distal portion of the tail has a dramatic effect on the organization of microtubules in the egg extract. After 30–60 min incubation, numerous microtubule asters were detected. Immunofluorescence with the anti-NuMA tail antibody revealed that the fusion protein was localized in the center of these asters (data not shown). (The same effect was observed when a fusion protein comprising the entire tail was used [data not shown].) However, the proximal portion of the tail was not able to induce the formation of these microtubule asters.

We then tried to examine whether NuMA affected microtubule organization by direct interaction with microtubules. Almost all microtubules polymerized from pure tubulin in the presence of the distal tail portion appeared

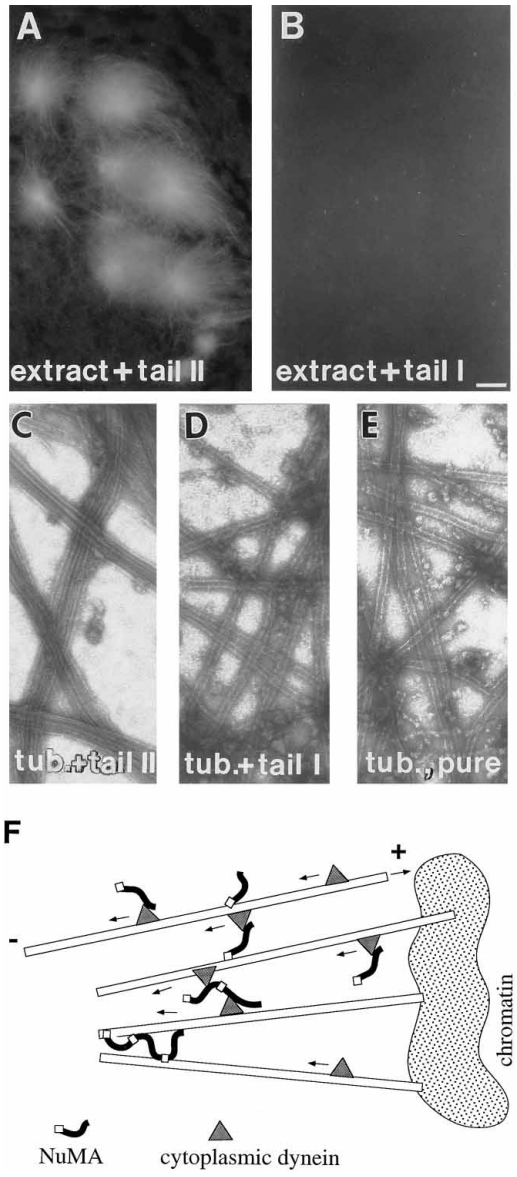

Figure 7. The Distal Portion of the NuMA Tail Has Microtubule-Binding Activity

Microtubule assembly in Xenopus egg extracts 60 min after addition of bacterial fusion proteins comprising (A) the distal tail region (tail II) or (B) the proximal tail region (tail I) of X-NuMA.

(C–E) Microtubules assembled in vitro from pure tubulin and (C) NuMA tail II, (D) NuMA tail I, or (E) no addition.

(F) Model of NuMA function during spindle assembly and pole stabilization. (Top) NuMA associates with cytoplasmic dynein; its binding to stationary microtubules enables the complex to translocate free microtubules towards the chromatin or, by binding to free microtubules, to move them polewards. (Middle) polewards moving complexes can act as zippers and induce the convergence of spindle microtubules. (Bottom) pole-accumulated NuMA can form a polymeric spindle pole matrix, stabilizing the spindle architecture and, together with dynein, acting as a counterbalancing force to chromosome-bound plus-end–directed microtubule motors.

highly bundled by electron microscopy (Figure 7C), whereas the proximal tail portion had no obvious morphological effect when compared with microtubules polymerized without additional protein (Figures 7D and 7E). We therefore conclude that a subdomain located between amino acids 1994 and 2253 in the NuMA tail has the ability to bind directly to α- or β-tubulin, a feature that may then induce or stabilize the bundling of microtubules as observed in spindle fibers and asters in vivo.

Discussion

NuMA Forms a Bifunctional Complex with Cytoplasmic Dynein That Is Required for Bipolar Spindle Formation

We have demonstrated that NuMA associates with the minus-end–directed microtubule motor cytoplasmic dynein and that the NuMA–dynein–dynactin complex is an essential component of mitotic spindle pole assembly. NuMA depletion eliminates bipolar spindle assembly, yielding aberrant structures with unusually long microtubules grouped around condensed sperm chromatin, lacking the normal fusiform shape of a spindle and lacking the known spindle pole proteins pericentrin and γ-tubulin. However, the chromatin is still located at the center of the aberrant microtubule array, equidistant from the microtubule ends. This raises the general question of the mechanism of spindle assembly in the egg extract. Centrosomal nucleation of spindle microtubules, as observed in animal cells, seems unlikely to occur in the depleted extracts because typical pericentriolar components, such as pericentrin and γ-tubulin, are missing from these structures, although the formation of microtubule asters in NuMA-depleted extracts seems to be unimpaired.

These findings offer direct experimental support for the view that chromatin itself may have the potential to organize preformed cytoplasmic microtubules into bipolar spindles without centrosomes involved, by the action of chromatin-bound plus-end–directed microtubule motors, as suggested by Karsenti and colleagues (Vernos and Karsenti, 1995; Hyman and Karsenti, 1996; Heald et al., 1996). As drawn in Figure 7F, focusing of the microtubules into spindle poles may then result from the activity of bifunctional minus-end–directed microtubule motors that interconnect parallel microtubules and induce their convergence by sliding towards the minus-end. Such a model requires an activity that creates at least two microtubule-binding sites, either by cross-linking two or more microtubule motor molecules (Verde et al., 1991; Heald et al., 1996) or by binding one motor to a different component that connects to microtubules by itself. Our finding that NuMA possesses microtubule-binding activity and associates nearly stoichiometrically with cytoplasmic dynein provides direct experimental evidence for the existence of such bifunctional complexes. As a result, these complexes could act as zippers and keep the polar microtubules tethered together (Vernos and Karsenti, 1995). This pathway might be followed for bipolar spindle formation in meiotic systems, such as Drosophila (Matthies et al., 1996) and Xenopus eggs, as well as during mitosis in plants, which assemble spindles without centrosomes.

Further, our demonstration that NuMA binds directly to microtubules offers strong evidence that once NuMA is concentrated at the poles, it acts as a spindle pole

matrix that maintains a stable spindle architecture by binding convergent microtubule fibers via its tail domain. In addition, the NuMA–dynein–dynactin complex may constrain the movement of microtubules away from the chromatin mass and maintain the size and the length of the spindle, as suggested by our NuMA-depletion/reconstitution experiments. A pole matrix component such as NuMA could provide sufficient mechanical stability by tethering parallel microtubule bundles. It could further explain the finding that spindles from which the centrosomes have been experimentally severed remain mechanically stable and even undergo poleward chromosome movement during anaphase (Nicklas et al., 1989; Nicklas, 1989). Moreover, in mitotic spindles such tethering is an attractive mechanism for anchoring spindle microtubules whose minus-ends are not embedded in the centrosome (it has been estimated that in some cells, 75% of interpolar spindle microtubules have their minus-ends more than 1 μm from the centrosome, at least during early anaphase of mitosis [Mastronarde et al., 1993]).

The model of NuMA/cytoplasmic dynein-dependent tethering of spindle microtubules into a pole is also consistent with the results obtained from microinjections of anti-NuMA antibodies (Kallajoki et al., 1991; Yang and Snyder, 1992; Gaglio et al., 1995) and anti-dynein antibodies into mitotic cells (Vaisberg et al., 1993), addition of anti-dynein antibody to in vitro assembled and spindles (Heald et al., 1996), and transfection studies with mutant forms of NuMA (Compton and Luo, 1995), all of which caused similar disorganization of spindles and dissociated spindle poles. The idea of NuMA forming a polymeric matrix that is involved in spindle microtubule organization is further supported by the recent findings of Saredi et al. (1996), who demonstrated that mutant NuMA lacking a nuclear localization signal forms fibrillar structures in the cytoplasm associated with tubulin. A polymeric form of NuMA, in association with microtubule motors, may constitute part of a highly dynamic spindle pole that can alter spindle morphology by regulating poleward microtubule flux (Sawin et al., 1992a; McNally et al., 1996). In this way, a flexible pole would be formed that could alter its shape during the cycle and provide morphological variability in spindles of different cellular systems (Mazia, 1987). Consistent with this view, meiotic spindles in mouse oocytes are characterized by the existence of barrel-shaped acentriolar spindles.

NuMA Is Not Involved in Microtubule Nucleation or Formation of Centrosomal Microtubule Asters

The localization of NuMA near the microtubule minus-ends in mitotic spindles and in taxol-induced microtubule asters (Maekawa et al., 1991; Kallajoki et al., 1992; Gaglio et al., 1995) fueled the initial speculation that NuMA might serve as a mitotic microtubule nucleator (Tousson et al., 1991; Kallajoki et al., 1992). Although an attractive hypothesis, this idea is not supported by in vivo observations in early prophase cells (Compton et al., 1992), where the nucleation of two sets of microtubule asters is seen before NuMA is released from the nucleus. More recently, Gaglio et al. (1995) have shown that taxol-induced microtubule asters, assembled without centrosomes in mitotic HeLa cell extracts, require the presence of NuMA where it appears to stabilize the astral microtubule array. In our experiments with Xenopus extracts capable of full spindle assembly, radial microtubule asters form from centrosomes without incorporation of NuMA (Figure 3A) as well as in depleted extracts in the absence of NuMA (Figure 5B). In whole extracts, only after prolonged incubation (30–40 min) does NuMA accumulate in the microtubule organizing center (Figure 3B), localizing asymmetrically at the minus-ends of those microtubule bundles connected to the sperm DNA. Concomitant with NuMA association, the morphology of the asters changes from a symmetric radial array into an asymmetric half-spindle–like array. The view most consistent with our evidence is that microtubule nucleation is initiated by centrosomal components other than NuMA and that NuMA itself is transported to the minus-ends of already preformed microtubules in association with cytoplasmic dynein, where it stabilizes parallel microtubule bundles (see model in Figure 7F).

Experimental Procedures

Cloning and Sequencing of X-NuMA

A λ-ZAP cDNA library from stage 26 Xenopus laevis tadpoles was screened using a ^{32}P-labeled DraI–EcoRI cDNA fragment (nucleotides 5337–7217) from human NuMA tail (Compton et al., 1992). DNA hybridization was performed according to Church and Gilbert (1984) at 65°C followed by washing in 0.1 × SSC, 1% SDS at 42°C. The library was rescreened using the 5′ sequences of this initial clone to identify a set of overlapping clones encoding most of X-NuMA. The 5′ most 218 nucleotides were identified by polymerase chain reaction–rapid amplification of cDNA ends (Frohman et al., 1988), using RNA from Xenopus A6 cells and an anti-sense primer to nucleotides 3508–3524. Sequencing was done using a Sequenase kit (USB, Cleveland, OH).

Immunological Procedures

Fusion proteins of X-NuMA rod and tail regions were expressed after cloning DNA fragments, encoding nucleotides 2074–3348 or 6173–7316 into vector pRSET C or B, respectively (Invitrogen, San Diego, CA), and transfection of the plasmid into BL-21 cells. Overexpressed fusion protein was purified over a Nickel-NTA agarose column (Qiagen, Chatsworth, CA). Fusion protein was dialyzed in PBS, mixed with Freunds adjuvant, and injected into rabbits. Sera were collected and affinity-purified over CNBr-Sepharose 4B columns coupled with the respective fusion proteins (Pharmacia, Uppsala, Sweden). Quantitation of immunoblots was performed by phosphorimaging, using known amounts of tail fusion proteins as standards and affinity-purified anti–X-NuMA tail antibody, followed by ^{125}I-protein A (DuPont/NEN, Boston, MA). Possible differences in the efficiency of blotting of the 35 kDa fusion protein and the 240 kDa X-NuMA were eliminated by dot-blotting identical amounts of extract and purified fusion protein directly onto nitrocellulose, followed by phosphorimaging.

Preparation of Egg Extracts and Immunodepletion Experiments

Mitotic (CSF–arrested) Xenopus laevis egg extracts and demembranated Xenopus sperm were prepared exactly as described by Murray (1991). For morphological assays, aliquots of rhodamine-tubulin were added to the extracts (Sawin and Mitchison, 1991). Demembranated sperm was added at a final concentration of 10^5 nuclei/ml to the extract to induce the formation of microtubule asters and spindles. The progress of aster formation and spindle assembly was monitored at all stages by fluorescence microscopy.

For the depletion of NuMA from the extracts, 60 μl of affinity-purified anti-tail antibody (0.2 mg/ml) were mixed with 30 μl slurry

of protein A-affiprep beads (Biorad, Hercules, CA) and incubated 1 hr to overnight. To remove unbound antibody, the beads were washed five times with 0.5 ml of PBS, once with 0.5 M NaCl in PBS, and finally twice more with PBS, and centrifuged, and as much liquid as possible was removed. To this pellet, an aliquot of 60 μl of CSF–arrested extract was added and rotated at 4°C for 1 hr. The beads were separated from the extract by quickly spinning the reaction tubes for 3 s at 2,000–3,000 rpm (approximately 700 × g) in a microfuge. The supernatant was collected and stored on ice until use. For every experiment, a control sample of mock-depleted extract was prepared, using rabbit anti-mouse serum (Sigma M-9637, St. Louis, MO) or another irrelevant antiserum (anti-FL2 against the lens-specific protein filensin [Gounari et al., 1993]). The degree of NuMA depletion was determined by immunoblotting and quantitation on a phosphorimager, as described above.

Bound protein was eluted from the protein A beads in 0.2 M glycine–HCl (pH 2.3), 0.5 M NaCl, after five washes with PBS plus 0.2% Triton X-100 and a brief high salt washing step with 0.5 M NaCl in PBS. In other experiments, an extraction buffer containing 60 mM KCl, 0.5 M NaCl, 15 mM Tris–HCl (pH 7.4), was used to elute NuMA-associated polypeptides for 20 min at room temperature, adapted from Madine et al. (1995). Immunoblotted protein was probed with anti-NuMA tail antibody, monoclonal anti-dynein intermediate chain antibody 70.1 (Steuer et al., 1990), monoclonal anti-dynactin antibody MAb 150 B (from Dr. T. Schroer, Baltimore, MD; see also Niclas et al., 1996), anti-dynein heavy chain antibody (Koonce et al., 1992), and anti–kinesin-like antibodies (anti–LAGSE and anti–HIPYR peptide antibodies, BABCO, Berkeley, CA). Dynein was enriched from frog egg extracts by Mg-ATP elution of taxol-stabilized microtubules formed in the extract (Verde et al., 1991; Niclas et al., 1996). Immunofluorescence of in vitro assembled spindles and nuclei was performed by mixing 20 μl aliquots of extract with 100 μl of 10 mM K–PIPES (pH 6.8), 0.3 M sucrose, 0.1 M NaCl, and 3 mM $MgCl_2$. The mixture was layered on top of a 5 ml cushion of 25% glycerol in the same buffer and centrifuged in a 15 ml corex tube onto a glass coverslip, mounted with a plastic adaptor, for 20 min at 6,500 rpm in an HS-4 swinging bucket rotor (Sorvall/DuPont, Newtown, Connecticut). Coverslips were fixed by immersion in −20°C cold methanol for 10 min. As primary antibodies for immunofluorescence, anti–X-NuMA tail, affinity-purified rabbit anti-pericentrin (Doxsey et al., 1994), or rabbit anti–γ-tubulin serum were used.

For reconstitution studies, antiserum was raised against a peptide of X-NuMA tail (MKRVSEESHYSPDTPEAKK), coupled with glutaraldehyde to keyhole limpet hemocyanin (Sigma). The serum was affinity-purified over NuMA-tail fusion protein and bound to protein A-affiprep beads. The beads were incubated with frog egg extract for 1 hr and subsequently washed three times with 60 mM KCl, 15 mM Tris–HCl (pH 7.4), 15 mM NaCl, twice with the same buffer containing 0.1% Triton X-100, and twice without detergent. NuMA was eluted from the antibody–protein A beads using an adapted protocol from Walczak et al. (1996) with a solution of the NuMA-tail peptide at 1 mg/ml in the washing buffer (without detergent) containing an additional 40 mM sodium borate, to raise the pH to 8.5. Elution was done at 4°C for 3–5 hr in a volume of 1 ml buffer for 100 μl of antibody–protein A beads. The eluate was concentrated to 10 μl in Nanospin Plus 100,000 MWCO-concentrator tubes (Gelman Sciences, Ann Arbor, MI) and washed in the same tubes in CSF–XB buffer (Murray, 1991). The concentrated proteins were analyzed on Coomassie-stained gels, and the amounts of NuMA for the reconstitution experiments were determined by quantitative immunoblotting, in comparison with the NuMA concentration in undepleted frog egg extract. Reconstitution experiments were performed by mixing one-tenth to one-fifth volume of immunoaffinty-purified NuMA with depleted mitotic frog egg extract and preincubating for 10 min at room temperature. Xenopus sperm DNA was then added and incubation continued for 1–2 hr. In a different set of reconstitution experiments, human NuMA was used that was purified from SF9 insect cells infected with human NuMA-encoding baculovirus (Gaglio et al., 1995).

Microtubule Bundling Assay

Fusion proteins containing X-NuMA residues 1994–2253 (tail II) and two additional tail-fusion proteins, representing a part of the rod domain and the proximal portion of the tail (residues 1719–1993; tail I) and the entire tail (residues 1719–2253) were prepared as described above. The purified proteins were dialyzed against PBS and diluted to a concentration of 0.2 mg/ml in egg extract containing rhodamine-tubulin. At various timepoints, samples were spotted onto a coverslip for fluorescence microscopy. The assay was repeated using the same proteins diluted into a solution of phosphocellulose-purified tubulin from bovine brain (2 mg/ml in 0.1 M PIPES (pH 6.9), 1 mM EGTA, 1 mM $MgCl_2$, 1 mM GTP). Samples were taken from 15–60 min, spotted onto carbon-coated copper grids, and negatively stained with 2% uranyl acetate for electron microscopy.

Acknowledgments

The authors would like to thank the following investigators for their generous donations of reagents: Dr. D. Compton (Dartmouth Medical School), who supplied recombinant human NuMA; and Dr. H. Joshi (Emory University), Dr. S. Doxsey (University of Massachusetts), Dr. M. Koonce (Wadsworth Center), and Dr. T. Schroer (Johns Hopkins University), who supplied antibodies to γ-tubulin, pericentrin, cytoplasmic dynein heavy chain, and cytoplasmic dynein intermediate chain and dynactin, respectively. We thank our colleagues in the laboratory, especially Dr. K. Wood, for help with the extract experiments; J. Thaler and Dr. J. Yucel for critically reading the manuscript; and Drs. A. Murray and T. Mitchison for advice on Xenopus extracts. This work was supported by a European Molecular Biology Organization long-term fellowship to A. M. and grant GM29513 from the National Institutes of Health to D. W. C.

Received April 19, 1996; revised September 3, 1996.

References

Church, G.M., and Gilbert, W. (1984). Genomic sequencing. Proc. Natl. Acad. Sci. USA *81*, 1991–1995.

Compton, D.A., and Cleveland, D.W. (1993). NuMA is required for the proper completion of mitosis. J. Cell Biol. *120*, 947–957.

Compton, D.A., and Luo, C. (1995). Mutation of the predicted p34 cdc2 phosphorylation sites in NuMA impair the assembly of the mitotic spindle and block mitosis. J. Cell Sci. *108*, 621–633.

Compton, D.A., Yen, T.J., and Cleveland, D.W. (1991). Identification of novel centromere/kinetochore-associated proteins using monoclonal antibodies generated against human mitotic chromosome scaffolds. J. Cell Biol. *112*, 1083–1097.

Compton, D.A., Szilak, I., and Cleveland, D.W. (1992). Primary structure of NuMA, an intraouclear protein that defines a novel pathway for segregation of proteins at mitosis. J. Cell Biol. *116*, 1395–1408.

Doxsey, S.J., Stein, P., Evans, L., Calarco, P.D., and Kirschner, M. (1994). Pericentrin, a highly conserved centrosome protein involved in microtubule organization. Cell *76*, 639–650.

Frohman, M.A., Dush, M.K., and Martin, G.R. (1988). Rapid production of full-length cDNAs from rare transcripts: amplification using a single gene-specific oligonucleotide primer. Proc. Natl. Acad. Sci. USA *85*, 8998–9002.

Gaglio, T., Saredi, A., and Compton, D.A. (1995). NuMA is required for the organization of microtubules into aster-like mitotic arrays. J. Cell Biol. *131*, 693–708.

Gill, S.R., Schroer, T.A., Szilak, I., Steuer, E.R., Sheetz, M.P., and Cleveland, D.W. (1991). Dynactin, a conserved, ubiquitously expressed component of an activator of vesicle motility mediated by cytoplasmic dynein. J. Cell Biol. *115*, 1639–1650.

Gounari, F., Merdes, A., Quinlan, R., Hess, J., FitzGerald, P.G., Ouzounis, C.A., and Georgatos, S.D. (1993). Bovine filensin possesses primary and secondary structure similarity to intermediate filament proteins. J. Cell Biol. *121*, 847–853.

Heald, R., Tournebize, R., Blank, T., Sandaltzopoulos, R., Becker, P., Hyman, A., and Karsenti, E. (1996). Self-organization of microtubules into bipolar spindles around artificial chromosomes in Xenopus egg extracts. Nature *382*, 420–425.

Hyman, A.A., and Karsenti, E. (1996). Morphogenetic properties of microtubules and mitotic spindle assembly. Cell *84*, 401–410.

Kallajoki, M., Weber, K., and Osborn, M. (1991). A 210 kDa nuclear matrix protein is a functional part of the mitotic spindle; a microinjection study using SPN monoclonal antibodies. EMBO J. *10*, 3351–3362.

Kallajoki, M., Weber, K., and Osborn, M. (1992). Ability to organize microtubules in taxol-treated mitotic PtK2 cells goes with the SPN antigen and not with the centrosome. J. Cell Sci. *102*, 91–102.

Kallajoki, M., Harborth, J., Weber, K., and Osborn, M. (1993). Microinjection of a monoclonal antibody against SPN antigen, now identified by peptide sequences as the NuMA protein, induces micronuclei in PtK2 cells. J. Cell Sci. *104*, 139–150.

Koonce, M.P., Grissom, P.M., and McIntosh, J.R. (1992). Dynein from Dictyostelium: primary structure comparisons between a cytoplasmic motor enzyme and flagellar dynein. J. Cell Biol. *119*, 1597–1604.

Lydersen, B.K., and Pettijohn, D.E. (1980). Human-specific nuclear protein that associates with the polar region of the mitotic apparatus: distribution in a human/hamster hybrid cell. Cell *22*, 489–499.

Madine, M.A., Khoo, C.Y., Mills, A.D., and Laskey, R.A. (1995). MCM3 complex required for cell cycle regulation of DNA replication in vertebrate cells. Nature *375*, 421–424.

Maekawa, T., Leslie, R., and Kuriyama, R. (1991). Identification of a minus end–specific microtubule associated protein located at the mitotic poles in cultured mammalian cells. Eur. J. Cell Biol. *54*, 255–267.

Mastronarde, D.N., McDonald, K.L., Ding, R., and McIntosh, J.R. (1993). Interpolar spindle microtubules in PtK cells. J. Cell Biol. *123*, 1475–1489.

Matthies, H.J.G., McDonald, H.B., Goldstein, L.S.B., and Theurkauf, W.B. (1996). Anastral meiotic spindle morphogenesis: role of the non-claret disjunctional kinesin-like protein. J. Cell Biol. *134*, 455–464.

Mazia, D. (1987). The chromosome cycle and the centrosome cycle in the mitotic cycle. Int. Rev. Cytol. *100*, 49–92.

McNally, F.J., Okawa, K., Iwamatsu, A., and Vale, R.D. (1996). Katanin, the microtubule-severing ATPase, is concentrated at centrosomes. J. Cell Sci. *109*, 561–567.

Murray, A.W. (1991). Cell cycle extracts. In Methods in Cell Biology, Volume 36, B.K. Kay and H.B. Peng, eds. (San Diego, California: Academic Press), pp. 581–605.

Niclas, J., Allen, V.J., and Vale, R.D. (1996). Cell cycle regulation of dynein association with membranes modulates microtubule-based organelle transport. J. Cell Biol. *133*, 558–593.

Nicklas, R.B. (1989). The motor for poleward chromosome movement in anaphase is in or near the kinetochore. J. Cell Biol. *109*, 2245–2255.

Nicklas, R.B., Lee, G.M., Rieder, C.L., and Rupp, G. (1989). Mechanically cut mitotic spindles: clean cuts and stable microtubules. J. Cell Sci. *94*, 415–423.

Saredi, A., Howard, L., and Compton, D.A. (1996). NuMA assembles into an extensive filamentous structure when expressed in the cell cytoplasm. J. Cell Sci. *109*, 619–630.

Sawin, K.E., and Mitchison, T.J. (1991). Mitotic spindle assembly by two different pathways in vitro. J. Cell Biol. *112*, 925–940.

Sawin, K.E., LeGuellec, K., Philippe, M., and Mitchison, T.J. (1992a). Mitotic spindle organization by a plus-end–directed microtubule motor. Nature *359*, 540–543.

Sawin, K.E., Mitchison, T.J., and Wordeman, L.G. (1992b). Evidence for kinesin-related proteins in the mitotic apparatus using peptide antibodies. J. Cell Sci. *101*, 303–313.

Schroer, T.A., and Sheetz, M.P. (1991). Two activators of microtubule-based vesicle transport. J. Cell Biol. *115*, 1309–1318.

Shamu, C.E., and Murray, A.W. (1992). Sister chromatid separation in frog egg extracts requires DNA topoisomerase II activity during anaphase. J. Cell Biol. *117*, 921–934.

Steuer, E.R., Wordeman, L., Schroer, T.A., and Sheetz, M.P. (1990). Localization of cytoplasmic dynein to mitotic spindles and kinetochores. Nature *345*, 266–268.

Tang, T.K., Tang, C.J.C., Chen, Y.L., and Wu, C.W. (1993). Nuclear proteins of the bovine esophageal epithelium: the NuMA gene gives rise to multiple mRNAs and gene products reactive with monoclonal antibody W1. J. Cell Sci. *104*, 249–260.

Tang, T.K., Tang, C.J.C., Chao, Y.J., and Wu, C.W. (1994). Nuclear mitotic apparatus protein (NuMA): spindle association, nuclear targeting and differential subcellular localization of various NuMA isoforms. J. Cell Sci. *107*, 1389–1402.

Tousson, A., Zeng, C., Brinkley, B.R., and Valdivia, M.M. (1991). Centrophilin: a novel mitotic spindle protein involved in microtubule nucleation. J. Cell Biol. *112*, 427–440.

Vaisberg, E.A., Koonce, M.P., and McIntosh, J.R. (1993). Cytoplasmic dynein plays a role in mammalian mitotic spindle formation. J. Cell Biol. *123*, 849–858.

Verde, F., Berrez, J.M., Antony, C., and Karsenti, E. (1991). Taxol-induced microtubule asters in mitotic extracts of Xenopus eggs: requirement for phosphorylated factors and cytoplasmic dynein. J. Cell Biol. *112*, 1177–1187.

Vernos, I., and Karsenti, E. (1995). Chromosomes take the lead in spindle assembly. Trends Cell Biol. *5*, 297–301.

Walczak, C.E., Mitchison, T.J., and Desai, A. (1996). XKCM1: a Xenopus kinesin–related protein that regulates microtubule dynamics during mitotic spindle assembly. Cell *84*, 37–47.

Yang, C.H., and Snyder, M. (1992). The nuclear–mitotic apparatus protein is important in the establishment and maintenance of the bipolar mitotic spindle apparatus. Mol. Biol. Cell *3*, 1259–1267.

Yang, C.H., Lambie, E.J., and Snyder, M. (1992). NuMA: an unusually long coiled-coil related protein in the mammalian nucleus. J. Cell Biol. *116*, 1303–1317.